JOURNAL OF MATERIALS SCIENCE 32 (1997) 6671–6680

Wear of engineering ceramics by a soft abrasive

J. T. CZERNUSZKA*, T. F. PAGE‡
Department of Metallurgy and Materials Science, University of Cambridge, Pembroke Street, Cambridge CB2 3QZ, UK

The wear behaviour of a number of engineering ceramics sliding against polyethyleneterephthalate (PET) has been examined. Microscopical examination of the worn surfaces has shown a wide distribution of size of grooves, from 50 nm to 1 μm. The smaller grooves seem to be made by anatase particles in the PET sheet. The larger grooves are made by particles ejected from the samples' surfaces by a fatigue mechanism. By relating the hardness of the engineering ceramics at a scale appropriate to the measured wear rates, some degree of agreement found. Further, it was found that the near-surface hardness of all the materials was lower than the macroscopic hardness values: the sole exception was anatase. Although the macroscopic hardness values of anatase were much lower than the alumina-based ceramics, the near-surface hardness values became relatively greater. In this way, what was originally thought to be a ''soft'' ceramic can now abrade a nominally ''harder'' one. The wear of the carbides is thought to be by an oxidation-assisted process.

1. Introduction

The mechanisms by which a material is removed from a hard surface when it is in sliding contact with a nominally softer abrasive are poorly understood and, until recently, sparsely investigated. This is, perhaps, unfortunate because many situations where ceramics are employed as wear-resistant surfaces would appear to fall within this category. Examples include ceramic–polymer couples as hip implants and ceramic cutting tool tips (e.g. [1, 2]). The major concern of this paper is the use of ceramics as guides during the manufacture of textile fibres. Although the wear resistances of the ceramic guides are superior to previously used materials, such as steel and porcelain, after a certain period they become sufficiently worn to warrant replacement. Worn or defective guides increase friction which results in non-reproducibility of fibre quality or even fibre damage and breakage. The aim of this study was to analyse possible materials for their suitability as replacements to existing fibre guides. Although it is known that the guides are given a special surface finish to achieve the desired frictional properties (e.g. [3]), this paper reports solely on the influence of materials' properties.

2. Wear mechanisms

There have been a few previous attempts at deducing the wear mechanisms applicable to the soft wear regime and they generally fall under two categories: (a) mechanical wear and (b) chemical wear. The following sections review each category in turn.

2.1. Mechanical wear

The concept of hardness as a parameter in wear arises from the relation of hardness to yield stress [4]. The action of an asperity or abrasive impinging on a surface may be likened to a sliding indentation process. The onset of plasticity occurs when the mean pressure is 1.1 Y, where Y is the yield stress of the material [5]. This implies a ratio in hardness values between abrasive and substrate of at least 0.9 for a substrate to plastically deform before the abrasive. However, it has shown that even if the indentor is nominally much softer than the substrate, plastic flow will occur in both materials [6]. For example, by repeatedly traversing a (soft) metallic slider over a single crystal of MgO it was possible to generate dislocations within a near-surface region of the MgO. Dislocation depths were independent of slider hardness, but dependent on load; the dislocation density increased to an asymptotic value with the hardness of the slider. After a critical number of traverses, fragmentation of the MgO occurred. The critical number of cycles to fragmentation decreased with an increase in hardness of the slider. It was suggested that the frictional forces at the sliding interface were (locally) greater than the critical resolved shear stress for dislocation generation and propagation. Wahl [7] first reported the effect of abrasive hardness on wear rate by showing that the volume of material removed increased with increasing hardness to a critical value, above which the wear rate remained nearly constant. This effect has been studied further [8] and it was concluded that when the ratio of annealed metal hardness, H_s, to that of the abrasive,

* *Present address*: Department of Materials, University of Oxford, Parks Road, Oxford, OX1 3PH, UK.
‡ *Present address*: Department of Mechanical Materials and Manufacturing Engineering, Division of Materials, The University of Newcastle upon Tyne, Newcastle upon Tyne, NE1 7RU, UK.

0022–2461

H_a, was greater the wear rate was very low. As the relative abrasive hardness increased, the wear rate rose and became constant when $0.6 < H_s/H_a < 0.7$. The fully strain-hardened hardness of the metal could be used instead, in which case it was found that the critical ratio was now about 0.8 [9]. In addition, it was found that, in some cases, wear did not become negligible until the ratio exceeded 1.2, indicating that some metal surfaces are worn by abrasives of lower hardness. This observation ties in with the results of Brookes and co-workers [6]. It has been suggested that anisotropy in hardness may be an important factor influencing relative wear rates [10]. This could mean that, even though on average the abrasive was softer than the substrate, there may be a degree of overlap depending on the orientation of the abrasive particle with respect to the substrate. Thus, for materials with a relatively small difference in average hardness values, similar mechanisms to wear by "hard" abrasives may occur. It is also possible that a material of low hardness may wear another of higher hardness by a brittle mechanism if their toughness values were different [11]. For example, copper sliding on alumina caused fracture of the alumina at relatively high loads [12].

2.2. Chemical wear

The high pressures (of the order of the indentation hardness) and possibly elevated temperatures at the sliding interface may enhance chemical reactions. For example, alumina abraded by SiC may react to form $SiC{\cdot}Al_2O_3$ [13], iron abraded by diamond formed cementite [14], and alumina worn by silica formed mullite [15]. These products would be weakly adhered to the parent surface and rapidly removed by subsequent contacts, causing material removal. If water is present in the system, as a lubricant or coolant, then alumina may hydrate to form gibbsite, boehmite or diaspore which again may be easily removed [16]. For non-oxide ceramics, there is the possibility of oxidation, for example titanium carbide and nitride tool materials [1].

3. Experimental procedure

3.1. Materials

The materials chosen for this study are described in Table I. The four de-based (i.e. glass-bonded) materials (HX, RG, FW and TE) are, or have been, used as guides in the textile industry and may be regarded as "standards" against which the others may be compared. HX, RG and FW are predominantly alumina, and TE is predominantly titania of the rutile crystal form [17]. The five single-phase aluminas (XA–XE) and the single-crystal sapphire were chosen to investigate the influence of grain size. The zirconia-based materials (CPSZ, MPSZ, YPSZ and ZTA) may be regarded as "high toughness" ceramics, and the SiC-based materials as "high hardness" ceramics. The glass was chosen as a relatively "soft" ceramic. These materials were chosen to span a range of mechanical properties (hardness and toughness) and microstructural properties (grain-size and phase distributions). Of the zirconia-based materials, CPSZ0 was in the unaged condition and consists predominantly of the cubic phase ($\sim$ 40 vol %), CPSZ64 has been peak-aged for maximum toughness and contains $>$ 50% tetragonal phase. CPSZ100 has been over-aged and contains a large proportion of monoclinic phase ($\sim$ 44 vol %). The ageing treatments were those used by Garvie *et al.* [18]. MPSZ was sub-eutectoid aged, giving rise to a grain-boundary monoclinic phase. This material has been suggested to have enhanced thermal shock properties [19]. YPSZ consists of $\gtrsim$80% tetragonal phase, the remainder being cubic zirconia. These results are tabulated in Table II.

3.2. Indentation hardness tests

Indentation tests were performed at room temperature over a range of loads. Vickers and Knoop profile

TABLE I Microstructural characterization

Acronym	Major phase	Additions	Grain size (μm)	Density (g cm^{-3})
HX	70% Al_2O_3	20% glass	$\sim$ 5	3.2
RG	75% Al_2O_3	15% glass	$<$ 5	3.45
FW	85% Al_2O_3	8% glass	$\sim$ 15	3.7
TE	90% rutile	$<$ 5% glass	1.5	4.1
XA	Al_2O_3	Single phase	1.2	3.57
XB	Al_2O_3	Single phase	10.0	3.61
XC	Al_2O_3	Single phase	18.0	3.77
XD	Al_2O_3	Single phase	21.0	3.79
XE	Al_2O_3	Single phase	35.0	3.85
Al_2O_3	Al_2O_3(10 12)	Single crystal	n/a	–
CPSZ0	ZrO_2	8% CaO	36	5.71
CPSZ64	ZrO_2	8% CaO	40	5.54
CPSZ100	ZrO_2	8% CaO	40	5.54
MPSZ	ZrO_2	5% MgO	40	5.54
YPSZ	ZrO_2	2.8% Y_2O_3	42	5.83
ZTA	Al_2O_3	40% ZrO_2	1.5	–
RL	SiC	10% Si	10	–
nSiC	SiC	SiC(0001)	N-trace	–
pSiC	SiC	SiC(0001)	Fe, Al trace	–
SLG	Soda–lime glass	n/a	n/a	–

TABLE II Phase distributions for the zirconia ceramics

Material	Volume fractions		
	Cubic	Tetragonal	Monoclinic
CPSZ0	32	59	8
CPSZ64	38	43	18
CPSZ100	46	10	44
MPSZ	22	54	25
YPSZ	8	82	–

indentors were used on a Leitz Miniload under ambient conditions. Loads between 1 kg and 5 g were used for an indentor dwell time of 10 s. At least ten indentations were made at each load for the Vickers indentations and at least 20 for the Knoop indentations. The resultant impressions were measured, either directly by light microscopy (LM) or, for the smallest indentations, by scanning electron microscopy (SEM). The SEM data were calibrated with the LM data for consistency.

3.3. Wear tests

Three sections of each material, approximately 5 mm thick, were cut with a high-speed annular diamond saw, carefully polished on a progressively finer succession of diamond-impregnated laps and cloths until flat, virtually featureless, surfaces were obtained. They were then etched in boiling orthophosphoric acid for a few minutes to remove any polishing damage, scrupulously rinsed in running water and finally ultrasonically cleaned in chloroethene. The polished samples were mounted in an equilateral triangular configuration in a brass jig, as shown in Fig. 1. The height of the specimens was adjusted to be as flat as possible and checked with a spirit level. Great care had to be taken at this stage to ensure reproducibility of the resultant wear. A polyethylene terephthalate (PET) sheet containing approximately 1.5 wt % anatase (approximately 0.5 μm diameter) was fixed to an aluminium plate on a metallographic polishing machine (see Fig. 1). A normal load of 1 kg was applied to the specimens and the rotation of the plate was set to be equivalent to a linear velocity of 1.4 m s^{-1}. The system was continuously lubricated with water at a rate of 1 l per 6 h. The specimens were "run-in" for 30 h prior to testing. To reduce the effects of degradation of the PET sheet a continuous run of 1 week was used to remove the original surface. To determine the thickness of material removed, each of the three specimens was indented at least three times with a Knoop indentor at a load of between 300 g and 1 kg, depending on the material. Prior tests on other, identically polished, samples were used to decide on the final load to be used. Too high a load resulted in lateral fracture, while too low a load made the impressions difficult to find and measure. These indentation diagonals were measured at intervals of 36 h. The volume of material removed was calculated from the difference in measured diagonal after a certain time (and knowing that the indentor:depth ratio is 30:1) multiplied by the nominal area of the specimens (which was held constant for each material, at 2.1×10^{-4} m^{-2}). Experiments were performed for at least eight time intervals. Prior to microscopic examination the surfaces were cleaned in boiling methanol to remove any adhered polymer. Microscopical examination of the worn surfaces was performed using a variety of techniques. Light microscopy (LM) was used with a Nomarski interference contrast (NIC) attachment to examine fine-scale features. Polarized reflected light microscopy (PRLM) would show sub-surface features such as cracks. The major technique employed, however, was scanning electron microscopy (SEM). The use of various imaging modes, such as secondary electron (SE), back-scattered electron (BSE) and cathodoluminescence (CL) imaging will be highlighted, as will the advantages of high-angle tilting to observe fine surface markings and stereo-imaging to obtain a three-dimensional representation of the worn surfaces.

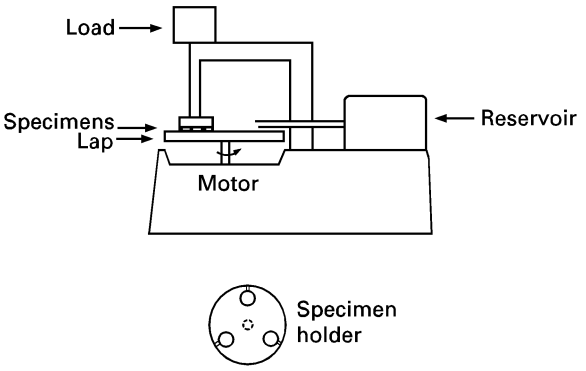

Figure 1 Schematic diagram of the wear rig.

4. Results

4.1. Indentation hardness tests

Fig. 2a shows the results of the indentation tests for the TE material for both Vickers and Knoop indentations. The results are plotted as a function of indentation depth because it has been previously established that the near-surface hardness and wear response are strongly dependent on environment [20, 21]. It is also thought to be more useful to compare hardness data with wear results if the scales of the contacts match [21, 22]. At high loads, and correspondingly greater penetration depths, the hardness tends towards an asymptotic value. As the scale is progressively reduced there is an increase in hardness, generally denoted by an indentation size effect index [23]. For shallow penetrations, typically less than 1 μm, there is a marked degree of softening. These results are similar to those for the other materials tested and the overall results are tabulated in Table III. The only exception to this general scheme was the hardness behaviour of the anatase shown in Fig. 2b. The Knoop hardness on a (1 0 0) surface was measured for two orientations. Along [0 0 1] the hardness behaviour versus load (or indentation depth) behaviour was similar to that observed for the other ceramics. However, along [0 1 1] the Knoop hardness does not reduce at low penetration

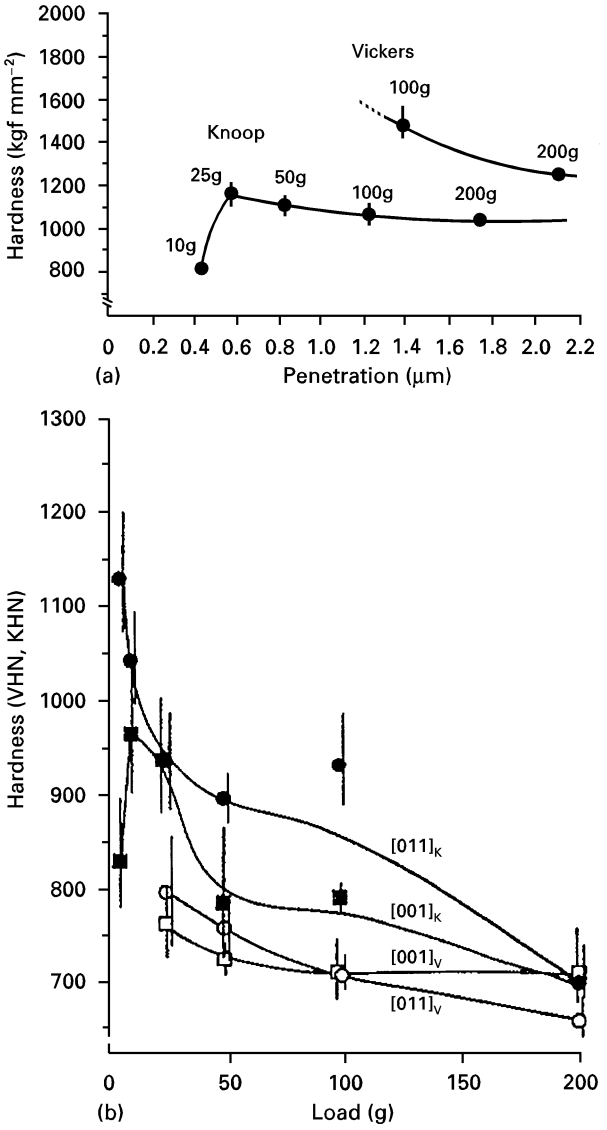

Figure 2 (a) Plot of hardness against penetration for TE using Knoop and Vickers profile indentors. (b) Hardness versus penetration for anatase along two directions on a (0 0 1) face. Shallower penetration occurs with Knoop indentors compared with Vickers indentors for the same load.

depths, but continues to increase to a final value of approximately 1100 kgf mm^{-2}. There is an approximately 50% increase in apparent hardness in reducing the indentor load from 200 g to 5 g. The low-load hardness of anatase along [0 1 1] can be greater than that of the alumina-based materials (HX, RG, FW, XA–XE, ZTA), except for the single-crystal alumina. It also possesses a higher hardness value than nSiC.

4.2. Wear tests

The results of the wear tests are presented in Table III, tabulated as wear resistance. For the experiments using water lubrication, all of the materials were examined; only three were used with the anatase slurry (these results are presented in the last column of Table III). Considering, initially, the water lubricated tests, the first point to note is that all these wear rates are very low, corresponding to a depth variation of approximately < 0.1 μm over a complete run. The accuracy of the indentation measurement technique is approximately 0.01 μm. The standard deviation of the results is typically 5% of the values stated in Table III.

TABLE III Hardness values at various indentation sizes and wear rates of the engineering ceramics

Material	Hardness (kgf mm^{-2})			Wear rate (10^{17} m^3 s^{-1})	
	Vickers		Knoop		
	1 kg load	10 μm	10 g load	Water	Slurry
HX	973	1374	716	17.2	
RG	1246	1388	590	12.2	
FW	1503	2234	580	1.88	
TE	1026	1086	815	9.09	270
XA	1100	1419	730	6.99	
XB	1543	1628	730	4.61	
XC	1704	1826	779	3.22	
XD	1586	1873	782	2.62	
XE	1434	2183	853	2.46	
Al_2O_3	1923	2177	2904	2.60	8.33
CPSZ0	1403	2143	1121	11.0	
CPSZ64	1250	1523	1683	4.18	
CPSZ100	912	1483	1150	10.0	
MPSZ	1178	1626	1192	52.7	
YPSZ	1101	1243	2210	2.06	
ZTA	1803	2018	884	3.30	
RL	1940	2125	2029	40.0	100
nSiC	2017	2483	800	90.0	
pSiC	3095	3498	1683	9.02	
SLG	590	620	537	23.8	
Anatase [0 0 1][a]	530	764	969	–	
[0 1 1][a]	482	812	1047	–	

[a] Anatase results were obtained using Knoop indentations only.

Taking each class of material in turn, the "standard materials" (viz. HX, RG, FW, and TE) are seen to exhibit a range of wear rates, with HX (an alumina-based material) having the highest wear rate and FW the lowest wear rate. The single-phase aluminas (XA–XE) have wear rates which decrease with increasing grain size, and decrease with increasing density (i.e. decreasing porosity). The single-crystal alumina has a slightly higher wear rate than XE. The wear rates for these materials lie between the values for RG and FW. The zirconia-based materials also exhibit a range of wear rates. Ageing the CPSZ materials for different times has altered the wear rates. YPSZ has the lowest wear rate of this class of materials. The silicon carbide-based materials have a spread of wear rates; nSiC has the highest wear rate of all the materials examined.

5. Discussion

5.1. Hardness tests

Some of the results of the hardness tests have been discussed previously [24, 25]. The effects of increasing hardness by decreasing the load are due in part to the interaction of the indentation-affected volume with microstructural parameters, such as grain boundaries and the necessity of a critical volume to initiate plastic flow [23, 26]. The first of these effects can be seen by comparing the single-phase aluminas, XA–XD (Table I with Table III) where the indentation size effect is more pronounced for the smaller grain-sized

material. This may be discerned by comparing the percentage variation between the hardness at a load of 1 kg and that at an indentation diagonal of 10 μm. The low load hardness (i.e. at a load of 10 g on a Knoop indentor) behaviour of all the materials to be worn was lower than the 10 μm hardness value. This near-surface hardness response is due to environmental effects [20, 21]. It is interesting to note that the two forms of titania, namely rutile (TE) and anatase, possess different near-surface hardness behaviour. TE has a surface softening effect while anatase has either a surface softening or surface hardening depending on orientation. It is not possible at this stage to develop any mechanism for this effect, but it must be due, in part at least, to the interactions of surface-adsorbed species with dislocations.

For the single-crystal SiC samples, the difference in hardness between nSiC and pSiC may be due to a doping effect on dislocation mobility [27]. For p-type material to be "harder" than n-type requires states associated with the dislocations to be towards the valence band, as is expected for germanium. Further details of this effect may be found in, for example, [27]. At the low-load end of the hardness data, surface effects will become more pronounced. Possible reasons for a near-surface softening effect are (a) that near-surface bending of the energy levels is occurring due to an adsorbed charge which makes the surface effectively more n-type (as has been observed for ZnO, see [28]), or (b) an amorphous, or very soft, surface oxide is present, or (c) a combination of both. The presence of a silicon–oxygen bonds was detected by infrared spectroscopy. It is likely that this factor predominates on the surface-softening effect. Indeed, hardness anisotropy experiments performed at loads of between 5 g and 10 g showed minimal hardness anisotropy implying a degree of surface disorder. Now, it is well known that doping a semiconductor may change the diffusion coefficient (see, for example, [29]). Indeed, this is the basis for the doping effect on dislocation mobility. So, in our case, the nSiC will have a higher diffusion coefficient than pSiC and so will oxidize much more. Consequently, it will have a thicker oxide layer and hence a lower surface hardness. This has an obvious corollary with the wear behaviour which will be discussed later.

5.2. Wear experiments

The results of the wear tests under water lubrication (Table III) will be discussed first of all in terms of their microstructures (Tables I and II) and then as a function of their hardness values, under different conditions of hardness measurement (Table III). The materials will be divided into: (a) those containing a glassy phase – the debased aluminas (HX, RG, FW), and the silica glass (SLG); (b) those containing silicon carbide – RL, nSiC, pSiC; (c) those based on zirconia – MPSZ, CPSZ0, CPSZ64, CPSZ100, YPSZ; (d) the single-phase aluminas – XA–XE and single-crystal alumina, Al_2O_3. The ZTA and TE samples do not fit easily into any category on microstructural terms, but will be included as appropriate. Throughout, microscopical techniques will be used to help ascertain the wear mechanisms.

5.2.1. The role of microstructure

The wear rates of the alumina-based guide materials (HX, RG and FW) in Table III decrease with an increase in proportion of glass phase (see Table I). In the extreme case, this is exemplified by SLG, the single-phase glass sample. This sort of behaviour would be expected if the grain-boundary glass phase was being worn away preferentially, leaving the crystalline surfaces standing proud. From Fig. 3a (which shows

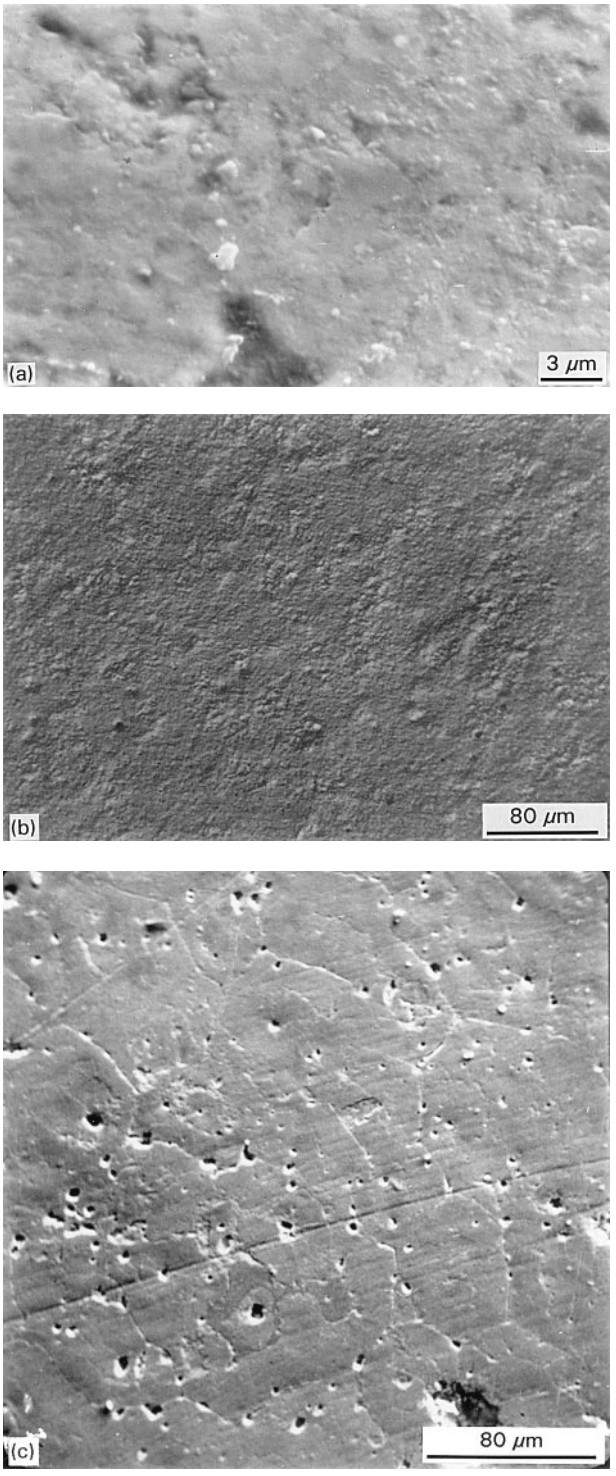

Figure 3 (a) SEM image of a worn TE surface, (b) NIC light micrograph of a worn MPSZ surface; (c) an SEM view of CPSZ100.

a worn surface of TE) there is a slight variation, although not very clear. Even so, any small grooves or scratches seem to traverse between phases with no apparent deviation. This point will be discussed further in Section 5.2.2. Occasionally, a few larger and deeper scratches were observed which were too large to be caused by the titania particles in the PET sheet. Possible causes of the formation of these wear grooves will also be discussed later (see Section 5.2.3).

The grain size of the "standard" materials was relatively small and this may be one reason why no clear differences between grains is shown. Fig. 3b shows an LM view, using Nomarski interferometer, of MPSZ. Subtle differences in height between adjacent grains are observed, as are the faint scratches running left to right across the sample. It appears, therefore, that there is an anisotropic effect in wear. A further effect was noticed with CPSZ100 (Fig. 3c). This material has a large proportion of monoclinic phase precipitated along the grain boundaries [30]. It appears as if this grain-boundary phase has been preferentially ejected resulting in a clear delineation of the grains.

The effect of second phases on the wear behaviour of the SiC-based materials was also examined. RL, the reaction-bonded material, contains approximately 10% free silicon from the processing route. Fig. 4 shows a scanning electron stereo-pair of worn RL. The use of stereo-pairs for examining worn surfaces has been highlighted previously [22]. The free silicon has been worn to a greater extent than the SiC. Careful examination of the surface shows further that the "new" SiC (shown as light grey) has worn more than the original grit (dark grey). It has been shown that the new SiC is more n-type than the original grit which tends to be p-type [31]. So, the n-type material with the lower hardness seems to have worn more than the "harder" original grit. The surface is also virtually scratch-free, in sharp contrast to the aluminas described above. As mentioned in Section 5.1, the nSiC is likely to oxidize more than pSiC [32] and this could well be the major material removal mechanism. Silicon oxidizes much more readily than SiC and consequently has worn away more quickly. Moreover, the depth to which the silicon has been removed is greater than that which could be reached by an anatase particle. This process has left the SiC grains standing proud of the surface, which would tend to increase the pressure and so enhance the wear rate of the SiC. It would seem likely that a balance between these two competing factors would occur.

To examine the effect of grain size and porosity on the wear rates of the alumina-based samples, the materials XA–XE, HX, RG, FW and Al_2O_3 will now be compared. All of these surfaces possessed similar appearances with generally only very shallow scratches visible on the surfaces, in a similar manner to TE (see Fig. 3). There did not appear to be any obvious relationship between grain size and wear rate, although there is a tendency for the larger grain size aluminas to exhibit the lower wear rates. A clearer relationship is obtained if the wear resistance is plotted versus density, see Fig. 5. A possible explanation for this is

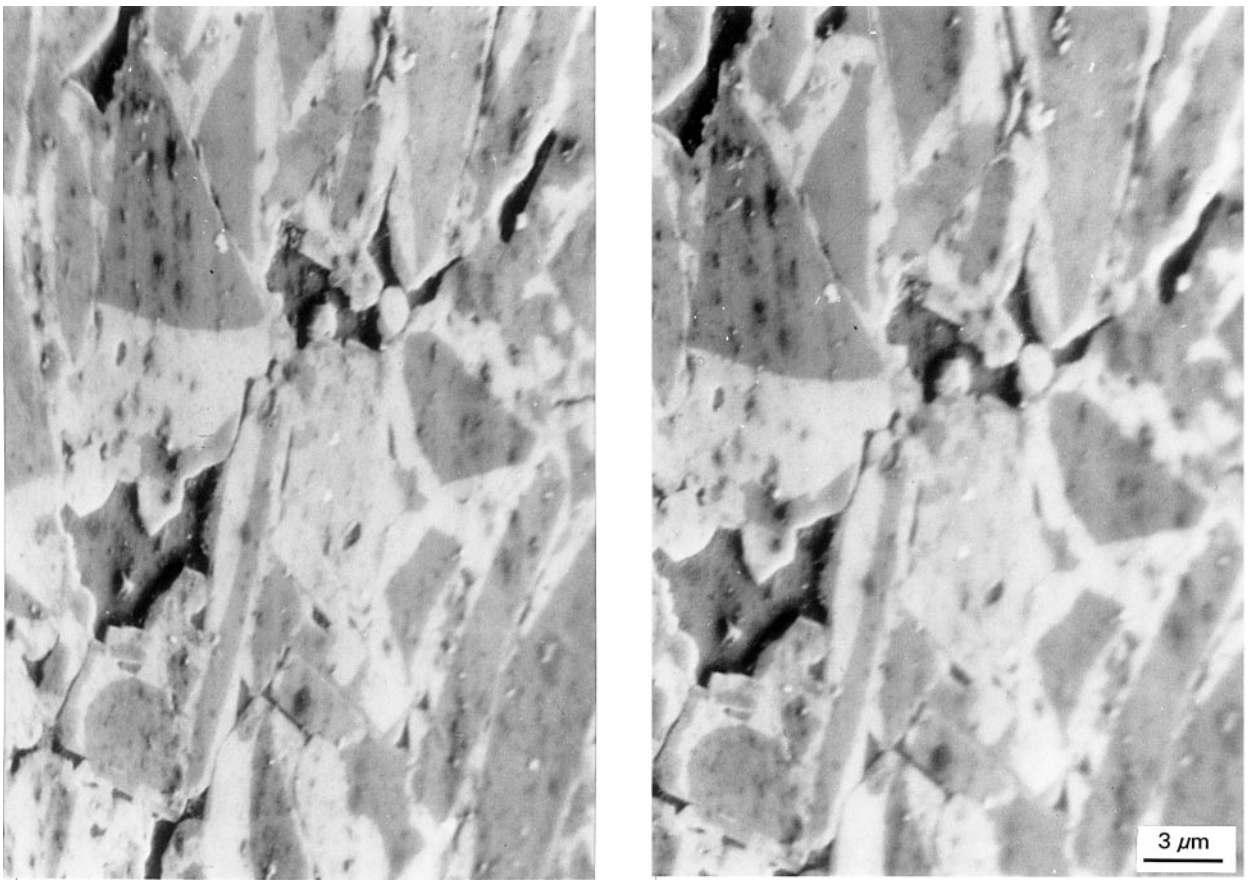

Figure 4 A stereo pair of a worn RL surface. Tilt axis vertical. Note that there is now considerable surface relief between the silicon (grey), the "new" SiC (light) and the "original" SiC grit (dark grey).

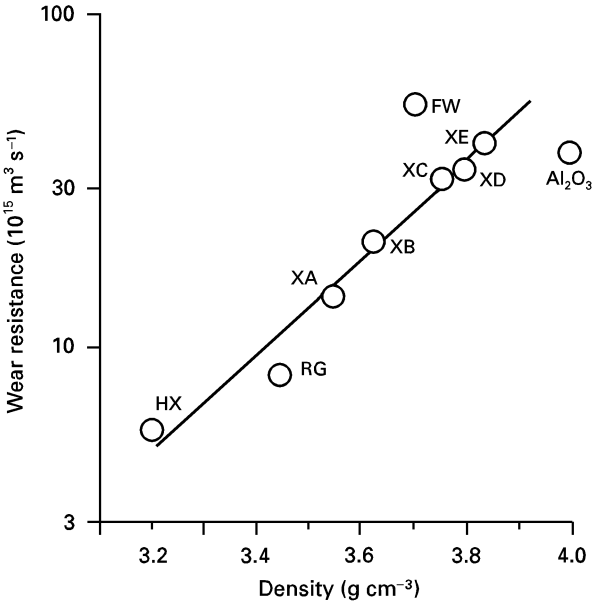

Figure 5 Plot of wear resistance of the alumina-based materials versus density.

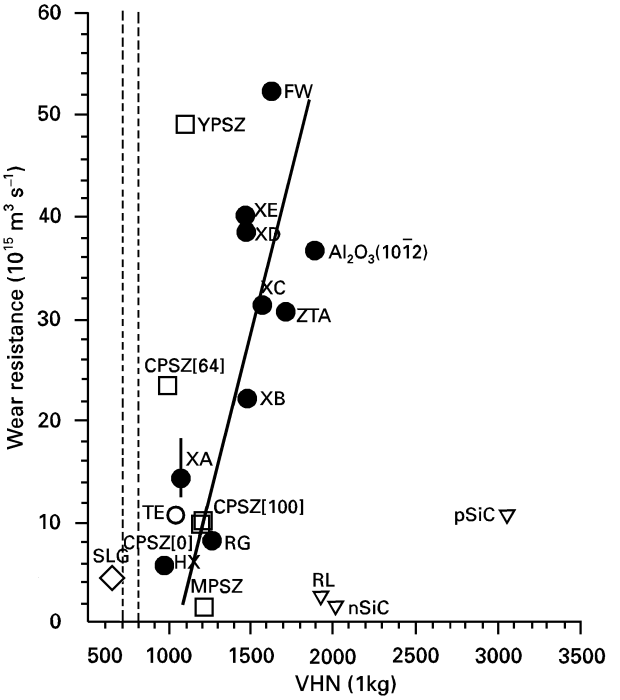

Figure 6 Plot of wear resistance versus Vickers hardness measured at a load of 1 kg.

through the relationship between density and volume fraction of porosity. It is well known that the relationship of Archard [33], purporting that contact pressure is independent of load, does not hold for polymers (e.g. [34]). This is because for polymers the actual area of contact is almost exactly the nominal area. Thus, it can be deduced that a decrease in density leads to an increase in area of surface pores and consequently an increase in contact pressure on the remaining alumina. This would help explain the behaviour of Fig. 5. How this behaviour may be modified by hardness variations will be discussed in the next section.

The behaviour of the zirconia-containing materials will now be discussed by comparing the wear-rate data of Table III with the microstructural data of Tables I and II. For the CPSZ ceramics, peak-ageing has resulted in a minimum in wear rate. YPSZ with the maximum amount of tetragonal phase has the lowest wear rate. It seems that the tetragonal phase suppresses material removal. Of the three polymorphs of zirconia the hardest is cubic, followed by tetragonal and the least hard is monoclinic [35]. So, hardness is not the only relevant wear parameter. The ZTA sample contained precipitates of predominantly tetragonal zirconia in an alumina matrix. Fig. 6 shows a scanning electron image which has been tilted to accentuate the surface topography parallel to the tilt axis. The brighter zirconia grains appear to be slightly proud of the surface. This suggests that the tetragonal zirconia has a greater wear resistance than the alumina. Indeed, YPSZ, consisting almost entirely of tetragonal zirconia, has an excellent wear resistance.

An overall SEM examination of the worn surfaces suggested that the width of the fine scratches on the surface varies from ≈ 50 nm up to ≈ 1 μm. There was a slight tendency for the SLG and TE (the two materials with the lowest nominal hardness values) to have larger scratches than the alumina-based and SiC-based materials. It is at this stage where we now need to turn to the complimentary hardness data.

5.2.2. The role of indentation hardness

It is common to try and relate wear rate data to hardness data and indeed this forms the basis of this paper. However, from the results of Section 4.1 and the discussion of Section 5.1 we must decide on which hardness scale, if any, to use for our comparisons. For the studies discussed here we will use the hardness calculated at a constant load of 1 kg, at a constant indentation diagonal of 10 μm and at a depth corresponding to the near-surface softened region. (This latter value will be approximated by using the hardness measured at a load of 10 g on a Knoop indentor, because the mean hardness values at 10 g and 5 g loads were similar and the 10 g load date had appreciably less scatter.)

A load of 1 kg is generally considered to be the maximum limit for a micro-hardness test. Indeed, severe radial and lateral fracture was observed for several specimens, notably SLG and HX. Because brittle fracture during wear was not a major problem we shall be concerned here solely with the plastic response of the materials (however, see Section 5.2.3).

Fig. 7 shows a plot of wear resistance versus hardness at a load of 1 kg. The dashed vertical lines correspond to the spread of hardness values which anatase has at this load. Typical error bars are only shown for XA to prevent cluttering the diagram. The hardness versus wear resistance behaviour follows no obvious pattern. For example, the wear resistances of SLG and pSiC are similar even though their respective hardness values are widely different. However, if the materials are grouped into four sets: alumina-based, zirconia-based, SiC-based and titania and glass, then some patterns do emerge. The SiC-based materials all possess low wear resistances (i.e. high wear rates). The alumina-based materials cover the entire range of

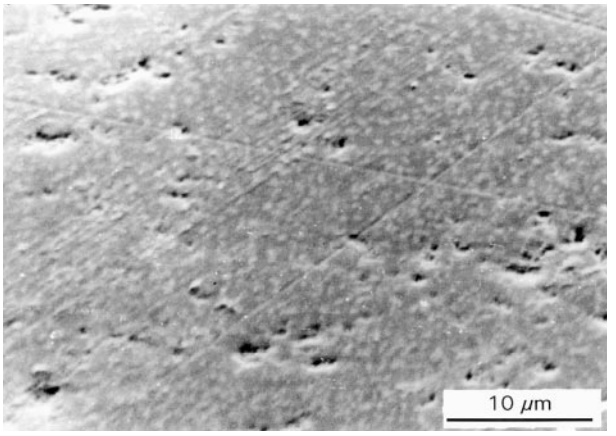

Figure 7 SEM image of worn ZTA. The bright regions are the zirconia precipitates in the darker alumina matrix.

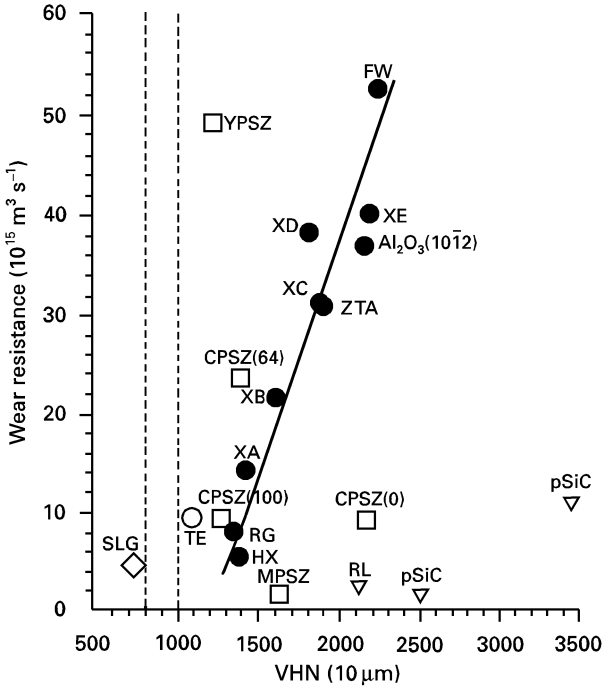

Figure 8 Plot of wear resistance versus Vickers hardness measured at an indentation diagonal of 10 μm.

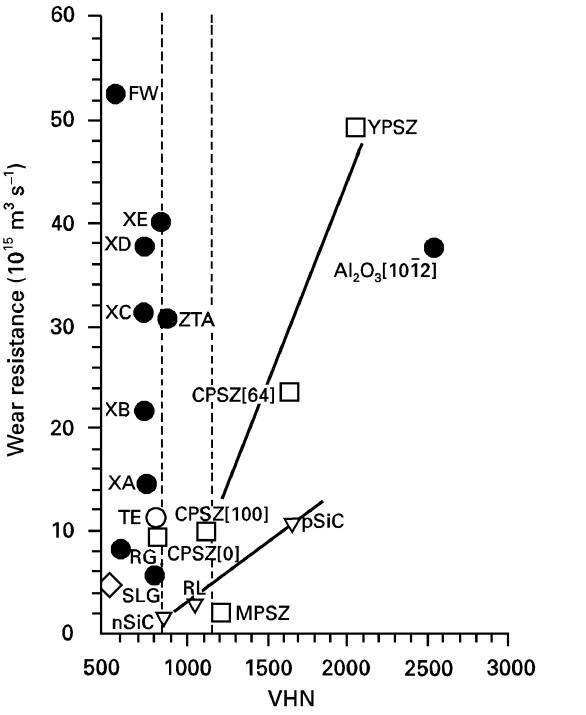

Figure 9 Plot of wear resistance versus Knoop hardness measured at a load of 10 g.

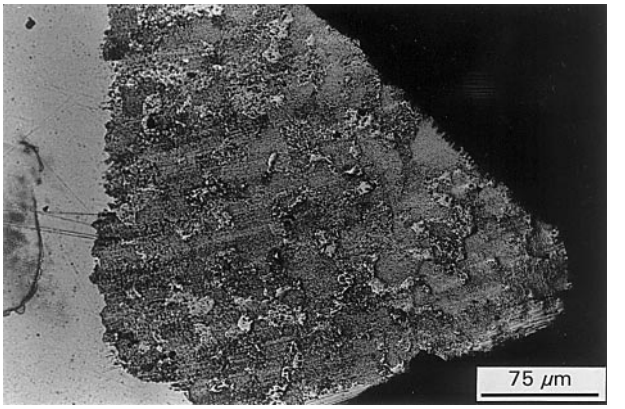

Figure 10 Light micrograph using Nomarski interferometry of a worn CPSZ0. Note the arrangement of transferred PET copying the underlying microstructure.

wear resistances with a trend for a linear relationship as indicated in Fig. 7. For the other groups, there is no clear trend. For example, YPSZ has a similar wear resistance to the best alumina materials (XE, FW and Al_2O_3). SLG was the only material with a lower hardness value than anatase and has a low wear resistance.

Fig. 8 presents the wear resistance data plotted against hardness measured at an indentation size of 10 μm. This hardness measure may be a more sensitive measure of the microstructural influences on hardness than a value at a particular load. By dividing the materials into the four groups again similar trends to Fig. 7 can be observed. In this case the alumina-based materials follow the linear relationship very closely (with a correlation coefficient of greater than 0.96). The other materials are even more widely scattered, though; in particular the zirconia-based materials.

It seems that neither measure of hardness mentioned above can successfully explain the wear behaviour. However, it has been noted previously that the near-surface hardness of the majority of these materials suffered a rapid decrease. The scale of the indentations over the range when this hardness drop occurs is the same as the width of the scratches observed during the wear experiments. Fig. 9 plots the wear resistance against the low-load hardness. There is now a good relationship between hardness and wear resistance for the zirconia-based and the SiC-based materials. That is, the correct order of wear resistance and hardness, as expected from conventional theories, is observed but only within each class of material. The alumina-based materials all suffer from this surface softening and the anatase now has a hardness value in excess of these materials (except for the single-crystal sapphire).

In fact, the hardness values of all alumina-based materials are now almost identical. This suggests that a similar softening mechanism is in operation for all the alumina samples. So, using the low-load hardness values helps to explain the zirconia-based and SiC-based materials but not the alumina-based materials.

5.2.3. Microscopical examination

One sample of CPSZ was misaligned during wear; the results from this experiment were not included in Table III. Transfer of PET to the ceramic surface was observed as shown in Fig. 10. The PET has reproduced the microstructure of the individual grains, that is anisotropic adhesion has occurred. Some of this transferred PET was examined in a TEM. A typical image is shown in Fig. 11. The TEM image shows a net-like configuration which is reminiscent of that observed at the intersection of crazes [36]. It is possible that the mechanism for polymer removal from the PET counterface is by crazing. The diffraction pattern was taken to show that there was no preferred alignment of the polymer film. It is common to get streaking of the diffraction pattern during wear of polymers showing preferred alignment along the sliding direction. This was not observed here.

On the majority of the samples the width of the grooves was found to vary into two broad groups: namely, very small < 50 nm and larger at approximately 200 nm across. The very fine scratches are attributable to the titania particles in the PET sheet. The larger scratches are much too large to be caused by the same mechanism and an alternative is proposed.

Fig. 12a shows a 1 kg Vickers indentation in TE. After the wear test the same indentation was examined, Fig. 12b. It should be noted that a lateral crack has been produced, presumably by a fatigue mechanism, and a relatively large amount of material has been removed from the surface. Even without an initial indentation to form a crack nucleus, a fatigue crack could form at a weak point, for example at a grain boundary or a pore. After a certain time grains

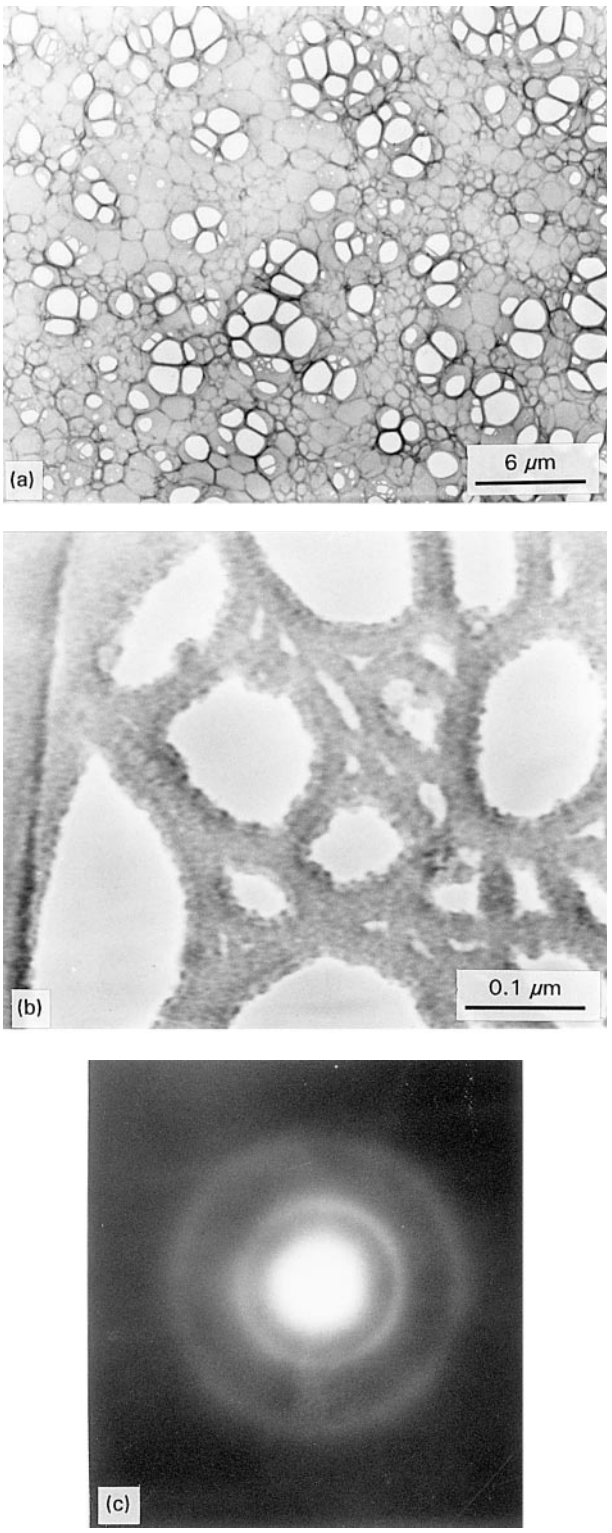

Figure 11 (a, b) TEM images of transferred PET film; (c) electron diffraction pattern.

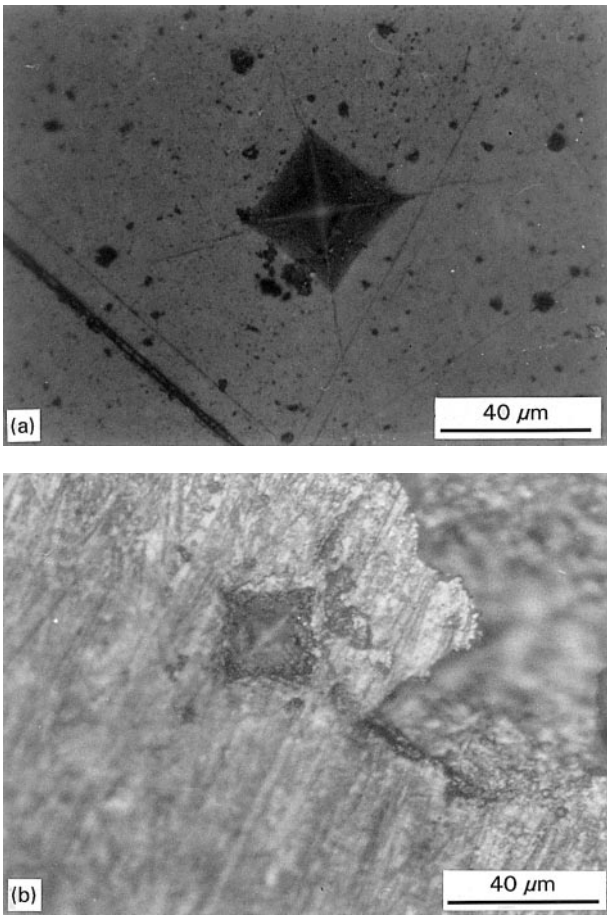

Figure 12 Reflected light micrograph of 1 kg Vickers indentation in TE. (a) No lateral cracking prior to the wear test; (b) break out of lateral cracking after the wear test.

could be ejected from the surface as wear debris. These sharp (and relatively large) wear particles could easily have given rise to the larger wear grooves. On a smaller scale this mechanism has led to the appearance of the CPSZ100 surface. In Fig. 6 the monoclinic phase has been ejected. This effect has been described previously by us for comparatively large-scale wear, i.e. by the interactions of deep grooves [22]. The importance of this effect has now been established but in terms of overall material removal its role is as yet unknown; and further experiments are in progress.

6. Conclusion

The hardness of oxide and carbide ceramics was found to be not constant with load. As the load is reduced from 1 kg to approximately 100 g the hardness increases. As the load, or to be more exact, the penetration of the indentor, is decreased further the hardness is decreased rapidly. The final value is strongly dependent on material. For example, zirconia-based materials which contain a large volume fraction of tetragonal phase do not have such a drastic near-surface reduction in hardness as cubic zirconias. For the SiC-based ceramics, this near-surface reduction is thought to be due to an oxide layer. For anatase, the near-surface hardness behaviour is dependent on crystallographic orientation. With the indentor aligned along [0 1 1] (1 0 0) the hardness does not decrease near the surface, but does with the indentor aligned along [0 0 1] (1 0 0). It was found that the anatase could have a hardness value greater than the alumina-based ceramics, irrespective of composition or grain size of the aluminas.

The wear behaviour of the ceramics has been analysed in terms of the near-surface hardness behaviour and some degree of agreement found. The zirconia-based and the SiC-based ceramics each had a linear response of hardness versus wear resistance. So, hardness has been shown to be a wear-related parameter for the wear of engineering ceramics by a nominally "soft" abrasive. Whether it is a direct parameter or an indirect one, for example a material with a higher hardness might have a lower oxidation/hydration rate, is not yet known.

Microscopical examination of the worn surfaces has shown a wide distribution of size of grooves – from 50 nm to 1 μm. The smaller grooves seem to be made by the anatase particles in the PET sheet. The larger grooves are made by particles ejected from the samples' surfaces by a fatigue mechanism. Evidence for this mechanism has been provided. This observation makes it difficult to ascribe definitely any single wear mechanism as being dominant in this set of wear experiments.

Acknowledgements

Professors R. W. K. Honeycombe and D. Hull are thanked for the provision of laboratory facilities. J.T.C. was in receipt of a SERC CASE award with ICI (Fibres) when this work was undertaken. Useful discussions with Frank Smith, P. E. Gallant and R. J. Merigold (all of ICI (Fibres)) are gratefully acknowledged.

References

1. P. A. DEARNELEY and G. M. TRENT, *Metals Tech.* **9** (1982) 60.
2. A. BEN ABDALLAH and D. TREHEUX, *Wear* **142** (1991) 43.
3. P. E. GALLANT and R. J. MERIGOLD, *J. Microsc.* **124** (1981) 275.
4. D. TABOR, *Br. J. Appl. Phys.* **7** (1956) 159.
5. A. G. ATKINS, in "The science of hardness testing and its research applications", edited by J. H. Westbrook and H. Conard (ASM, OH, 1973) p. 223.
6. C. A. BROOKES and M. P. SHAW, *Nature* **263** (1976) 760.
7. H. WAHL, *Metalen* **9** (1954) 4.
8. M. M. KRUSCHOV and M. A. BABICHEV, *Russ. Engng J.* **44** (1964) 43.
9. R. C. D. RICHARDSON, *Wear* **11** (1968) 245.
10. E. RABINOWICZ, in "Wear of materials", edited by K. C. Ludema (ASME, New York, 1983).
11. A. G. EVANS and D. B. MARSHALL, in "Fundamentals of friction and wear", edited by D. A. Rigney (ASM, OH, 1981) p. 439.
12. D. H. BUCKLEY, NASA Tech. Memo TMX-68046 (1972).
13. E. D. DOYLE and S. K. DEAN, NBS Special Publication 562 (National Bureau of Standards, Washington, DC, 1979) p. 107.
14. M. P. HITCHENER and J. J. WILKS, *Wear* **93** (1984) 63.
15. E. J. DUWELL and H. C. BUTZKE, *ASLE Trans.* **7** (1964) 101.
16. O. IMANAKA and M. OKATOMI, NBS Special Technical Publication 562 (National Bureau of Standards, Washington, DC, 1979) p. 157.
17. N. K. GIBBS, PhD thesis, University of Cambridge (1982).
18. R. C. GARVIE, R. R. HUGHES and R. T. PASCOE, in "Materials Science Research", Vol. 2, edited by H. Palmour, R. F. Davis and T. M. Hare (Plenum Press, 1984).
19. R. J. HANNINK, *J. Mater. Sci.* **18** (1983) 457.
20. R. E. HANNEMAN and J. H. WESTBROOK, *Philos. Mag.* **18** (1967) 73.
21. J. T. CZERNUSZKA and T. F. PAGE, *J. Mater. Sci.* **22** (1987) 3973.
22. *Idem*, *J. Microsc.* **140** (1985) 159.
23. P. M. SARGENT and T. F. PAGE, *Proc. Br. Ceram. Soc.* **26** (1978) 209.
24. J. T. CZERNUSZKA and T. F. PAGE, *ibid.* **34** (1984) 145.
25. *Idem*, *J. Mater. Sci.* **22** (1987) 3907.
26. S. J. BULL, T. F. PAGE and E. H. YOFFE, *Philos. Mag. Lett.* **59** (1989) 281.
27. P. B. HIRSCH, *J. Microsc.* **118** (1980) 3.
28. J. T. CZERNUSZKA, *Inst. Phys. Conf. Ser.* **104** (1989) 315.
29. W. FRANK, V. GOSEL, M. MEHRER and A. SEEGER, in "Diffusion in crystalline solids", edited by G. E. Murch and A. S. Nowick (Academic Press, 1984) Ch. 2.
30. J. T. CZERNUSZKA and T. F. PAGE, *J. Mater. Sci.* **27** (1992) 1683.
31. J. N. NESS, PhD thesis, University of Cambridge (1987).
32. N. W. JEPPS, PhD thesis, University of Cambridge (1987).
33. J. F. ARCHARD, *J. Appl. Phys.* **24** (1953) 981.
34. J. J. BIKERMAN, *Polym. Sci. Technol.* **5** (1974) 601.
35. R. STEVENS, "An introduction to zirconia", Magnesium Elektron Publication 113 (1986).
36. A. F. YEE, W. V. OLSZEWSKI and S. MILLER, in "Toughness and brittleness of plastics", edited by R. D. Deanin and A. M. Crugnola (ACS, Washington, 1976) Ch. 6.

Received 14 November 1994
and accepted 15 March 1995